Research Square

Preprints are preliminary reports that have not undergone peer review. They should not be considered conclusive, used to inform clinical practice, or referenced by the media as validated information.

Effects of Renewable Diesel Exhaust on Lung Function and Self-rated Symptoms for Healthy Volunteers in a Human Chamber Exposure Study

Louise Gren (louise.gren@design.lth.se)
Lund University: Lunds Universitet https://orcid.org/0000-0002-1198-4995

Katrin Dierschke
Lund University: Lunds Universitet

Fredrik Mattsson
Lund University: Lunds Universitet

Eva Assarsson
Lund University: Lunds Universitet

Annette M. Krais
Lund University: Lunds Universitet

Monica Kåredal
Lund University: Lunds Universitet

Karin Lovén
Lund University: Lunds Universitet

Jakob Löndahl
Lund University: Lunds Universitet

Joakim Pagels
Lund University: Lunds Universitet

Bo Strandberg
Lund University: Lunds Universitet

Martin Tunér
Lund University: Lunds Universitet

Yiyi Xu
University of Gothenburg: Goteborgs Universitet

Per Wollmer
Lund University: Lunds Universitet

Maria Albin
Karolinska Institute: Karolinska Institutet

Jörn Nielsen
Lund University: Lunds Universitet

Anders Gudmundsson

Lund University: Lunds Universitet
Aneta Wierzbicka
Lund University: Lunds Universitet

Research

Keywords: hydrotreated vegetable oil (HVO), inhalation, aerosol, peak nasal inspiratory flow (PNIF), peak expiratory flow (PEF), forced oscillation technique (FOT), symptoms, pulmonary function, non-road vehicles, occupational exposure limits (OELs)

Posted Date: April 16th, 2021

DOI: https://doi.org/10.21203/rs.3.rs-405371/v1

License: This work is licensed under a Creative Commons Attribution 4.0 International License.
Read Full License

Effects of renewable diesel exhaust on lung function and self-rated symptoms for healthy volunteers in a human chamber exposure study

Louise Gren[1,2], Katrin Dierschke[3], Fredrik Mattsson[1], Eva Assarsson[3], Annette M. Krais[3], Monica Kåredal[2,3], Karin Lovén[1, 2], Jakob Löndahl[1,2], Joakim Pagels[1,2], Bo Strandberg[3], Martin Tunér[4], Yiyi Xu[5], Per Wollmer[6], Maria Albin[3,7], Jörn Nielsen[3], Anders Gudmundsson[1,2], Aneta Wierzbicka[1*]

Keywords: hydrotreated vegetable oil (HVO), inhalation, aerosol, peak nasal inspiratory flow (PNIF), peak expiratory flow (PEF), forced oscillation technique (FOT), symptoms, pulmonary function, non-road vehicles, occupational exposure limits (OELs)

[1]Ergonomics and Aerosol Technology, Lund University, Lund, SE-221 00, Sweden

[2]Lund University, NanoLund, SE-221 00 Lund, Sweden

[3]Division of Occupational and Environmental Medicine, Lund University, Lund, SE-221 85, Sweden

[4]Division of Combustion Engines, Lund University, Lund, SE-221 00, Sweden

[5]School of Public Health and Community Medicine, Institute of Medicine, University of Gothenburg, Sweden

[6]Department of Translational Medicine, Lund University, Sweden

[7]Unit of Occupational Medicine, Institute of Environmental Medicine, Karolinska Institute, Stockholm, Sweden

*Corresponding author (published version): aneta.wierzbicka@design.lth.se

Corresponding author during revision process: Louise Gren, louise.gren@design.lth.se

Abstract

Background: Diesel engine exhaust causes adverse health effects. Meanwhile, the impact of renewable diesel exhaust on human health is less known. In this study, nasal patency, pulmonary function, and self-rated symptoms were assessed in 19 healthy volunteers after two separate 3-hour exposures to renewable diesel (hydrotreated vegetable oil [HVO]) exhaust, and exposure to filtered air (FA) for comparison. The HVO exposures were generated with two modern non-road vehicles (2019) having either: 1) no aftertreatment system (HVO_{PM+NOx}), or 2) an aftertreatment system containing a diesel oxidation catalyst and a diesel particulate filter (HVO_{NOx}). The exposure concentrations complied with current EU occupational exposure limits (OELs) of NO, NO_2, formaldehyde, polycyclic aromatic hydrocarbons (PAHs), and future OELs of elemental carbon (EC) from 2023.

Results: Exposure to HVO_{PM+NOx} consisted of PM1 (≈90 µg m^{-3}, 54 µg m^{-3} EC) and NO_x (NO 3.4 ppm, NO_2 0.6 ppm). The average total respiratory tract deposition of PM1 was 27 µg h^{-1}. The deposition fraction of HVO PM1 was 40-50% higher compared to diesel exhaust PM1 from an older vehicle, due to smaller particle sizes of the HVO_{PM+NOx} exhaust. Exposure to HVO_{NOx} consisted mainly of NO_x (NO 2.0 ppm, NO_2 0.7 ppm) with low level of PM1 (~1 µg m^{-3}). Compared to filtered air, exposure to HVO_{PM+NOx} and HVO_{NOx} caused higher incidence of self-reported symptoms (78%, 63%, respectively, vs. 28% for FA, $p<0.03$). Especially, exposure to HVO_{PM+NOx} showed 40-50% higher eye and throat irritation symptoms. Compared to filtered air, a decrement in nasal patency was found for the HVO_{NOx} exposures (-18.1, 95%CI: -27.3 to -8.8 L min^{-1}), and for the HVO_{PM+NOx} (-7.4 (-15.6 to 0.8) L min^{-1}). Overall, no change was indicated in the pulmonary function tests (spirometry, peak expiratory flow, forced oscillation technique), except a slight increase in FEV_1/FVC after exposure to HVO_{NOx}.

Conclusion: Short-term exposure to HVO exhaust below the EU OELs did not cause severe pulmonary function changes in healthy subjects. However, an increase in self-rated mild irritation symptoms, and mild decrease in nasal patency after two HVO exposures may indicate irritative effects from exposure to HVO exhaust from modern non-road vehicles below future OELs.

Introduction

Exposure to petroleum diesel engine exhaust is known to cause adverse health effects (1–4), and since 2012, diesel engine exhaust has been classified as carcinogenic to humans (5). Several human exposure studies have linked diesel exposure to acute health effects, among them short-term reduced lung function (6–10), airway inflammatory responses (10–13), irritation symptoms (6,7,14,15), and cardiovascular effects (16–18). Stricter emission standards in recent years and improved emission reduction techniques have reduced the particle and gas emissions from modern diesel vehicles. At the same time the use of renewable diesel fuels has increased rapidly in an effort to reduce net CO_2 emissions. These fuels, such as hydrotreated vegetable oil (HVO) and biodiesel of fatty acid methyl ester (FAME) types, decrease the particulate matter (PM) emissions compared to petroleum diesel (19–22). However, compared to petroleum diesel the toxicity of these emissions is less evaluated. Only a few controlled human exposure studies of FAME type fuels exist (8,23), while there are to the best of the authors' knowledge, no such studies on HVO. Compared to FAME fuels, HVO is the preferred fuel for full substitution (pure biodiesel, B100) of petroleum diesel in non-modified diesel engines due to its greater engine compatibility. With all the known adverse effects of petroleum diesel exhaust from older vehicles, the research focus should be directed to investigate the health effects of realistic exposure concentrations from modern renewable fuels used in vehicles with different exhaust aftertreatment systems.

The exhaust emissions of HVO are, on the one hand, similar to petroleum diesel as the combustion generates carbonaceous PM ("soot"), nitrogen oxides (NO_x), polycyclic aromatic hydrocarbons (PAHs), etc., but on the other hand, they are different in terms of concentration, particle size and chemical composition (24–27). For example, HVO can decrease the PM emission by 20-50% in comparison to petroleum diesel (20,21). It should be noted that similar to diesel, HVO contains no oxygen or feedstock-derived impurities (e.g., metals) that influence emission characteristics, as do FAME-type biodiesels. The aerosol emission characteristics thus differ for HVO and FAME

86 compared to petroleum diesel (22,28). The solid PM fraction of the exhaust from diesel and HVO
87 is dominated by soot, which can be measured thermo-optically as elemental carbon (EC). A new
88 EU occupational exposure limit (OEL) for diesel engine exhaust, measured as EC, of 50 μg m^{-3} (29)
89 will be implemented in 2023 to reduce the exposure of the 3.6 million workers within the member
90 states (30). Because estimates of the life-time mortality risk from occupational exposure to diesel
91 for cancer alone (not including myocardial infarction or COPD) indicate that exposure levels need
92 to be kept extremely low (Vermeulen et al. 2014), it is of key importance to identify potential
93 adverse effects of the substitutes. As the substitution of petroleum diesel by renewable diesel is
94 increasing, a considerable number of people will be exposed to its exhaust. It is hence of interest to
95 understand the potential health effects of exhaust exposure from engines running on HVO, while
96 complying with the future OELs.
97
98 Exhaust aftertreatment systems are used in diesel vehicles in order to reduce the environmental
99 and health hazardous emissions of PM (both mass and number concentration), CO, NO_x, and
100 organic compounds such as PAHs. An aftertreatment system can, for example, contain a diesel
101 oxidation catalyst (DOC) that oxidizes CO and organic compounds (31,32), and a diesel particle
102 filter (DPF) that oxidizes soot particles which removes significant amounts of PM (33). Hence use
103 of aftertreatment systems should reduce exposure to such emissions and their associated health
104 effects. However, a recent review assessing the effects of DPFs' use on health impacts in
105 occupational settings did not present conclusive results (34). It is thus of interest to investigate the
106 health impact from vehicles with different degrees of emission reduction technology.
107
108 Due to improved engine operation, modern diesel engines with or without aftertreatment systems
109 generally emit lower concentrations of pollutants (35) and reduce exhaust particle mass and size
110 (36). Particle characteristics such as size and morphology are of key importance in considering
111 possible health effects, as these characteristics determine where in the lungs the particles will

112 deposit. The deposition pattern in the lung depends on multiple aerosol characteristics and not
113 solely on the respirable PM mass concentration (37).
114
115 In the present study we investigate the human health effects from exposure to exhaust from two
116 modern non-road vehicles (wheel loaders). Due to their engine capacity, they fall under different
117 emission standards and were equipped with 1) no external aftertreatment device, or 2) a DOC in
118 combination with a DPF. The different emissions aftertreatment allowed for a comparison of the
119 exposure to NO_x from diesel engines with and without a particulate fraction and other gaseous
120 pollutants. We aimed to evaluate self-rated symptoms, nasal patency, and pulmonary function
121 after exposure to HVO exhaust from modern non-road vehicles that complied with the EU OELs.
122 Additionally, we investigated the lung deposition of HVO exhaust particles with the deposition of
123 petroleum diesel from an older light-duty vehicle presented by Wierzbicka et al. in a previous
124 study (15).
125

Results

Main findings

We compared the effects of exposure to exhaust from hydrotreated vegetable oil (HVO) (a renewable diesel fuel) with filtered air (FA). The vehicle without an external aftertreatment system (HVO_{PM+NOx}) generated emissions of PM, NO_x and organic compounds. The vehicle with an external aftertreatment consisting of a DOC and DPF (HVO_{NOx}) emitted NO_x with only negligible concentrations of particles and measured organic components (hereafter referred to only NO_x). The two exposures to HVO caused mild self-rated irritations symptoms. 44% reported eye irritation symptoms during the HVO_{PM+NOx} exposure. The number of volunteers who reported throat irritation symptoms was a factor 4.5 and 4 higher for HVO_{PM+NOx} and HVO_{NOx} respectively, compared to FA. In comparison to FA exposure, nasal obstruction (lower PNIF) occurred for the HVO_{NOx} exposure. In the first of the following two sections we describe the exposure aerosol characteristics and the HVO exhaust particle deposition in the airways in relation to diesel exhaust particles. In the second, we describe the health effects in terms of self-rated symptoms and airway function.

Exposure and lung deposition

Exposure aerosol characteristics

A summary of the average aerosol exposure concentrations and characteristics are presented in Table 1. The average aerosol exposure characteristics during the three exposure scenarios are presented in Fig. 1. The average PM1 concentration during the HVO_{PM+NOx} exposures was 93±13 µg m^{-3} and the average particle number (PN) concentration was $3.0 \cdot 10^5 \pm 0.3 \cdot 10^5$ cm^{-3} (Table 1). In contrast, during HVO_{NOx} and FA exposures, the average exposure concentrations of PM1 were ~1 µg m^{-3} and PN <100 cm^{-3} (Table 1). For HVO_{PM+NOx}, the elemental carbon (EC) fraction of total carbon was 66±3% corresponding to an average EC concentration of 54±6 µg m^{-3} (Table 1). The

152 two vehicles were operated in a similar load/idle sequence, which is seen as increasing (during
153 load) and decreasing (during idle) PM1 mass (Fig. 1a) and NO concentrations during HVO_{PM+NOx}
154 exposure, and increasing/decreasing NO_2 levels for the HVO_{NOx} exposures (Fig. 1b).
155
156 The NO and NO_2 concentrations were comparable for the two HVO exposures (no vehicle had
157 external NO_x removal devices, such as selective catalytic reduction [SCR]) and on average below
158 the 8-hour OELs. During the HVO_{NOx} exposure, the average NO_2 was slightly higher and the
159 average NO lower compared to HVO_{PM+NOx} (Table 1). The variations in NO and NO_2 from the
160 load/idle operation as described above can be seen in Fig. 1b. In addition, NO increased rapidly
161 after the cold start at the start of the HVO_{NOx} exposure and decreased shortly thereafter when the
162 diesel oxidation catalyst (DOC) of the vehicle has reached the operating temperature and started to
163 convert NO to NO_2 more efficiently.
164
165 During the HVO_{PM+NOx} exposure scenario (with the vehicle without aftertreatment) gas-phase
166 organic compounds were quantified, but below the OELs, among them PAHs (889±53 ng m^{-3}),
167 BTEX (11.6±3.0 µg m^{-3}), and formaldehyde (51±6 µg m^{-3}). These emissions were low or below limit
168 of detection (LOD) during the other exposure scenarios. Full PAH (33 native and alkylated, 10 oxy-
169 and 17 nitro-PAHs) and BTEX analyses are presented in Additional file B and C, respectively.
170
171 The particle number and mass size distribution of HVO_{PM+NOx}, together with the effective density
172 of the soot agglomerates, are shown in Fig. 2a. The effective density decreased with increasing
173 mobility size, as the soot agglomerates became more open in their structure, and the diesel soot
174 power law function described by Park et al. (38) could be fitted to the experimental data (Fig. 2a).
175 The mass mobility exponent (D_{fm}) was on average 2.3 (where 3 corresponds to perfect spheres). An
176 example of the soot agglomerates generated during the HVO_{PM+NOx} exposure is imaged by

transmission electron microscopy (TEM) in Fig. 2b. The average primary particle diameter of the soot agglomerates of HVO_{PM+NOx} was 24.5 ± 7.3 nm and an example is marked in Fig. 2b.

Table 1. Summary of the average aerosol concentrations and characteristics during exposures in the chamber.

		HVO_{PM+NOx}	HVO_{NOx}	FA
Particle phase	PM1 (µg m^{-3}) (*Gravimetric*)	93 ± 13	~1[a]	~1[a]
	PM1 Total Carbon (TC, µg m^{-3})	82 ± 10	<1	<1
	EC/TC (%)	66 ± 3	-	-
	OC/TC (%)	34 ± 3	-	-
	PM1 (µg/m^3) (*SMPS* and ρ_{eff})	81 ± 9	0.0 ± 0.0	0.5 ± 0.5
	PM2.5 (µg m^{-3}) (extrapolated fit)	*81 ± 9*	-	-
	GMD_{mass} (nm)	114	-	-
	GSD_{mass} (nm)	1.48	-	-
	PN (cm^{-3})	$3.0 \cdot 10^5$	$9.0 \cdot 10^1$	$7.1 \cdot 10^1$
	PN std. dev	$0.3 \cdot 10^5$	$4.1 \cdot 10^1$	$4.3 \cdot 10^1$
	GMD_{PN} (nm)	71	47.2	-
	GSD_{PN} (nm)	1.64	1.46	-
	Surface area (cm^{-2} cm^{-3})	$9.5 \cdot 10^{-5}$	-	-
	Surface area std. dev (cm^{-2} cm^{-3})	$1.4 \cdot 10^{-5}$	-	-
	Particle phase PAHs[b] (ng m^{-3})	43 ± 3	0.3 ± 0.7	0.2 ± 0.2
Gas phase	Gas phase PAHs[b] (ng m^{-3})	850 ± 48	97 ± 11	116 ± 29
	Formaldehyde (µg m^{-3})	51 ± 6	<8	<8
	Sum BTEX (µg m^{-3})	7.9 ± 2.5	1.7 ± 0.3	1.3 ± 0.1
	VOCs (ppb)	333 ± 69	11 ± 5	<10
	NO (ppm)	3.4 ± 0.1	2.0 ± 0.1	<0.001
	NO_2 (ppm)	0.57 ± 0.04	0.70 ± 0.04	<0.001
	NO/NO_2 ratio	5.7	2.9	-
	CO_2 (ppm)	1344 ± 143	1332 ± 135	813 ± 140

All values are the average of all exposures (n=5-6) of a given type with ± 1 std. dev. Full compound analyses of PAHs and BTEX are found in Additional file B and C, respectively.
[a] There were large uncertainties in the gravimetric mass analysis at low/no mass concentrations. The mass concentrations were in the range of the blank filters (-1±3 µg).
[b] 33 native and alkylated, 10 oxy- and 17 nitro-PAHs were included in the analysis.

Inhaled deposited fraction and dose

184 The calculated average inhaled deposited particle mass from nasal breathing during the
185 HVO_{PM+NOx} exposure in the tracheobronchial and alveolar regions, from airway generation 1 to 24,
186 is presented in Fig. 3a. Deposited doses are given as deposited mass (µg) and as deposited mass
187 per lung tissue area (ng cm^{-2}). The mass dose is largest in the distal airways (airway generations
188 >10), but when expressed as deposited mass per lung tissue area the largest dose is found in the
189 upper tracheobronchial region (airway generation <10). No deposition was analyzed for HVO_{NOx}
190 due to low PM and PN concentrations (Table 1).
191
192 A comparison is presented in Fig. 3b of the total deposited particle mass doses in the different
193 airway regions in the current study and in a previous petroleum diesel exposure study (6,15). The
194 comparison was made for both the original diesel mass concentration in the past study (276 µg m^{-}
195 ^{3}, light grey bars) and with the same mass concentration as in this study (93 µg m^{-3}, dark grey bars)
196 using the original aerosol characteristics of the petroleum diesel (MMD 195 nm, GSD 1.65). The
197 deposited mass of the diesel aerosol was higher in comparison to $HVO_{PM+NOx,}$ but lower when using
198 the same exposure mass concentrations. The deposited fractions of the HVO_{PM+NOx} aerosol mass
199 (i.e., the fraction of the deposited mass compared to the total inhaled mass concentration) were
200 around 40-50% higher compared to petroleum diesel in the tracheobronchial and alveolar regions.
201 The average accumulated deposited dose in the respiratory tract was 82 µg for HVO_{PM+NOx},
202 corresponding to an hourly average of 27 µg h^{-1}.
203
204 The inhaled deposited dose depends on multiple lung parameters (FRC, tidal volume, breathing
205 pattern, etc.). For additional comparison with petroleum diesel, the same deposition model (oral
206 breathing, [39]) was used as in Wierzbicka et al. (15). Table 2 presents the deposited HVO_{PM+NOx}
207 particle dose expressed as mass, number and surface area compared to the petroleum diesel
208 exposure (using the original exposure concentrations). Please note the three times higher particle
209 mass concentration in the case of diesel in comparison to HVO when looking at values of deposited

dose by mass. The mass (and surface area) deposition fraction was a factor 1.5 higher for HVO_{PM+NOx} than diesel. Additionally, the deposited dose in terms of particle number was a factor 1.2 higher for HVO_{PM+NOx}. As the particle number concentration was higher for HVO_{PM+NOx}, despite the lower mass concentration, this led to a higher number of particles deposited in the lungs for HVO compared to diesel. The deposited mass fractions differ slightly from the multiple-path particle dosimetry (MPPD) model due to model characteristics, see Additional File D for a comparison of the deposition fraction depending on particle size for the two models.

Table 2. The average lung deposition (oral breathing) fractions of PM1 of HVO_{PM+NOx} and petroleum diesel.

		HVO (PM1)	Diesel (PM1), Wierzbicka et al. 2014	Unit
Mass concentration (µg m^{-3})		93 ± 13	276 ± 56	
Particle number concentration (µg m^{-3})		$3.0 \cdot 10^5 \pm 0.3 \cdot 10^5$	$3.9 \cdot 10^5 \pm 0.5 \cdot 10^5$ *	
Surface area concentration (µg m^{-3})		$9.5 \cdot 10^{-5} \pm 1.4 \cdot 10^{-5}$	$3.5 \cdot 10^{-4} \pm 0.7 \cdot 10^{-4}$	
Mass	Deposited fraction	0.40 ± 0.004	0.27 ± 0.01	
	Deposited dose during 3h exposure	100.4 ± 12.4	118.5 ± 21.6	*µg*
Number	Deposited fraction	0.52 ± 0.002	0.45 ± 0.03	
	Deposited dose during 3h exposure	$4.3 \cdot 10^{11} \pm 5.2 \cdot 10^{10}$	$2.8 \cdot 10^{11} \pm 3.5 \cdot 10^{10}$	*Particles*
Surface area	Deposited fraction	0.40 ± 0.004	0.27 ± 0.01	
	Deposited dose during 3h exposure	104.5 ± 12.9	151.9 ± 27.7	*cm^2*

The average lung deposition (oral breathing) fractions of PM1 of HVO_{PM+NOx} was calculated with the model presented by Rissler et al. (39) and compared to the calculated deposited doses of petroleum diesel from Wierzbicka et al. (15). The average mass, particle number and surface area concentrations of the respective exposures are given. All values are presented as mean ± 1 std. dev.
*PM0.5

Health effects

Self-rated symptoms

The number of volunteers reporting symptoms from eye, throat, nose, and chest during the exposures are shown in Table 3. Exposure to HVO (HVO_{PM+NOx} and HVO_{NOx}) caused significantly higher incidences of reported symptoms compared to FA (78%, 63% vs. 28%, $p<0.03$ for both). The proportion of volunteers who reported throat irritation was a factor 4.5 and 4 higher for HVO_{PM+NOx} and HVO_{NOx}, respectively, compared to FA. The difference was statistically significant for HVO_{PM+NOx} ($p=0.011$) and with borderline significance for HVO_{NOx} ($p=0.062$). The proportion of reported eye irritation symptoms was around a factor 2.5 higher for HVO_{PM+NOx} compared to FA with a borderline significance ($p=0.07$). No volunteers reported chest tightness during the FA exposure, while a few individuals did so during the HVO_{PM+NOx} and HVO_{NOx}, respectively. However, it should be noted that the reported symptom scores were generally low (mostly below 10 in a 0-100 VAS) for all categories.

Table 3: Descriptive table of the reported symptoms during each exposure scenario.

	Any reported symptom			Eye [a]			Throat [b]			Nose [c]		Chest [d]	
	Yes/total	%	P (χ^2-test)	Yes/total	%	P (χ^2-test)	Yes/total	%	P (χ^2-test)	Yes/total	%	Yes/total	%
FA	5/18	28%	-	3/18	17%	ref	2/18	11%	ref	1/18	6%	0/18	0%
HVO_{NOx}	12/19	63%	0.031	7/19	37%	0.27 [e]	8/19	42%	0.062 [e]	2/19	11%	1/19	5%
HVO_{PM+NOx}	14/18	78%	0.003	8/18	44%	0.07	9/18	50%	0.011	5/18	28%	3/18	17%

Descriptive table of the number of volunteers reporting any type of symptoms, symptoms categorized by type, and χ^2-tests for any reported symptoms, eye and throat symptoms. The χ^2-tests are compared to the FA exposure. χ^2-tests were not performed for nose and chest symptoms due to the low number of reported symptoms. The number of subjects was 19 for HVO_{NOx} and 18 for FA and HVO_{PM+NOx}.
[a] Itching, running and/or sore eyes. [b] Sore/dry/irritated throat. [c] Running nose and/or nose congestion. [d] Chest tightness/breathlessness. [e] P values obtained from Fisher exact test.

Airway function

Peak nasal inspiratory flow (PNIF) and peak expiratory flow (PEF)

The changes in ΔPNIF and ΔPEF at each time point during the exposure are shown in Fig. 4, and absolute values are presented in Additional file E. For both PNIF and PEF, there was an increasing trend throughout the FA exposure while no such increase was seen for neither of the two HVO

243 exposures. The differences between average changes in PNIF and PEF measurements (ΔPNIF and
244 ΔPEF) during the two HVO exposure scenarios compared to FA are presented in Table 4. Although
245 no decrease in absolute PNIF values was found for the HVO exposures, we observed a statistically
246 significant decrement in ΔPNIF during HVO_{NOx} exposure compared to the FA exposure (-18.1 L
247 min^{-1}, $p \leq 0.001$), and a borderline significant decrement during HVO_{PM+NOx} exposure (-7.4 L min^{-1},
248 p=0.08). No difference in ΔPEF was found between the HVO exposures and FA.
249
250 Table 4: The average changes in ΔPNIF and ΔPEF (L min^{-1}) during each exposure scenario and
251 compared to the FA exposure.

	PNIF			PEF		
	estimated mean (95%CI)	beta (95% CI)	p-value	estimated mean (95%CI)	beta (95% CI)	p-value
FA	10.3 [4.1, 16.6]	Ref	ref	2.2 [-5.1, 9.5]	Ref	ref
HVO_{NOx}	-7.7 [-14.4, -1.1]	-18.1 [-27.3, -8.8]	<0.001	-2.5 [-10.2, 5.3]	-4.6 [-15.6, 6.3]	0.40
HVO_{PM+NOx}	2.9 [-3.4, 9.1]	-7.4 [-15.6, 0.8]	0.08	4.7 [-2.4, 11.9]	2.5 [-7.1, 12.2]	0.60

Estimated average changes in ΔPNIF and ΔPEF (L min^{-1}) during each exposure scenario (estimated mean) and differences between the two HVO exposures and FA exposure (beta). The beta values (L min^{-1}) and significance (p-value) are based on the linear mixed model with exposure order correction. Values within brackets are the 95% CI.

252
253 *Spirometry*
254 The result of the FVC (forced vital capacity), FEV_1 (forced expiratory volume in one second) and
255 FEV_1/FVC (in L, z-score and as % of predicted) is presented in Additional file F. FEV_1 and FVC
256 showed minimal and statistically insignificant differences after all exposure scenarios (Additional
257 file F1). A minimal (from 0.81 to 0.82) but statistically significant ($p<0.05$) increase in mean
258 FEV_1/FVC was found after the HVO_{NOx} exposure. Compared to FA, no significant changes were
259 found after the HVO exposures (Additional file F2).
260
261
262 *Oscillometry parameters*

263 The results of the oscillometry parameters reflecting reactance (X_5, A_X, F_{RES}) and resistance (R_5,
264 R_{19}) are presented in Table 5. There was no statistically significant difference before and after any
265 exposure for any parameter (median). Weak statistical evidence (p=0.084) was found for a
266 decrease in reactance (X_5) after HVO_{NOx}; however, similar trends were not seen for the related
267 parameters of A_X and F_{RES} which downplays the probability of a physiological effect on the lung.
268 Some volunteers had baseline oscillometry values deviating from the normal range (40,41) but
269 with normal spirometry measures; thus, the volunteers were further categorized into a "typical"
270 and "atypical" group based on their oscillometric measures (Additional file A). The atypical group
271 showed a higher proportion of having a history of symptoms and atopy (80% vs. 54%, $p<0.05$).
272 They were hypothesized to be more sensitive and have a different lung reaction to the exposures
273 than the typical group. However, no significant interactions between the typical/atypical groups
274 and PNIF or PEF were found. Neither were any statistically significant changes found for any
275 oscillometry parameters of the atypical/typical groups after the HVO exposures in comparison to
276 FA.
277
278 Table 5. The average lung reactance (X_5, A_X), resistance (R_5, R_{19}, R_{5-19}) and resonant frequency
279 (F_{RES}) before and after exposure and the paired test.

	Exposure	Before exposure		After exposure		Related-Samples Wilcoxon Signed Rank Test
		median (25%, 75%)	mean (Std. D)	median (25%, 75%)	mean (Std. D)	p-values
R_5 ($cmH_2O\ s\ L^{-1}$)	FA	3.56 (3.28, 4.16)	3.66 (0.87)	3.86 (3.17, 4.31)	3.82 (1.07)	0.215
	HVO_{NOx}	3.75 (2.86, 4.74)	3.98 (1.33)	3.87 (3.13, 4.86)	4.17 (1.67)	0.494
	HVO_{PM+NOx}	3.61 (3.1, 4.68)	4.06 (1.67)	3.6 (2.93, 5.22)	4.10 (1.84)	0.845
R_{19} ($cmH_2O\ s\ L^{-1}$)	FA	3.09 (2.63, 3.77)	3.11 (0.73)	3.24 (2.67, 3.71)	3.20 (0.71)	0.286
	HVO_{NOx}	3.12 (2.56, 3.96)	3.21 (0.74)	3.33 (2.68, 3.88)	3.28 (0.83)	0.355
	HVO_{PM+NOx}	3.14 (2.61, 3.82)	3.17 (0.86)	3.03 (2.54, 3.97)	3.26 (1.00)	0.215
R_{5-19} ($cmH_2O\ s\ L^{-1}$)	FA	0.38 (0.2, 0.72)	0.54 (0.51)	0.51 (0.16, 0.68)	0.63 (0.69)	0.5
	HVO_{NOx}	0.79 (0.18, 1.11)	0.77 (0.80)	0.72 (0.24, 0.98)	0.88 (1.08)	0.212
	HVO_{PM+NOx}	0.49 (0.22, 1.07)	0.89 (1.05)	0.5 (0.27, 1.15)	0.84 (1.04)	0.948

X_5 ($cmH_2O\ s\ L^{-1}$)	FA	-1.19 (-1.34, -1.1)	-1.25 (0.40)	-1.16 (-1.38, -0.99)	-1.35 (0.71)	0.306
	HVO_{NOx}	-1.21 (-1.45, -0.88)	-1.3 (0.65)	-1.22 (-1.53, -1.1)	-1.49 (1.02)	0.084
	HVO_{PM+NOx}	-1.15 (-1.86, -1.07)	-1.58 (1.12)	-1.19 (-1.51, -0.99)	-1.43 (0.96)	0.102
A_X ($cmH_2O\ L^{-1}$)	FA	5.9 (4.16, 8.72)	7.44 (5.00)	5.63 (2.75, 8.79)	7.85 (6.66)	0.913
	HVO_{NOx}	5.99 (3.34, 14.13)	9.24 (7.91)	6.31 (3.19, 13.14)	10.73 (13.13)	0.658
	HVO_{PM+NOx}	6.33 (4.26, 15.31)	12.14 (15.50)	5.52 (3.44, 13.97)	12.00 (17.05)	0.586
F_{RES} (Hz)	FA	15.38 (13.59, 19.47)	16.28 (3.88)	15.64 (12.9, 18.88)	15.93 (4.41)	0.528
	HVO_{NOx}	14.88 (12.91, 23.66)	17.36 (5.90)	14.88 (12.97, 22.96)	17.61 (5.98)	0.494
	HVO_{PM+NOx}	16.22 (12.28, 22.05)	17.64 (5.91)	14.98 (13.56, 19.71)	17.58 (7.18)	0.744

Discussion

We present the effects of the first controlled human chamber exposure to exhaust from renewable diesel fuel, namely, hydrotreated vegetable oil (HVO). Modern non-road vehicles with or without an aftertreatment system were used to investigate the health effects from two different but realistic exposures: 1) PM combined with NO_x and, 2) NO_x alone, both of which were compared to filtered air (FA) exposure. The exposure levels were designed to be close to, but below the current EU 8-hour OELs for NO, NO_2, BTEX and PAHs (naphthalene and benzo(a)pyrene), and the future EU OEL for elemental carbon (EC, from 2023).

We found that exposures to HVO exhaust caused mild irritation symptoms compared to FA. Additionally, the observed PNIF patterns indicate that nasal obstruction occurred for both HVO exposures compared to FA. However, no overall changes in pulmonary function measured as PEF, spirometry or forced oscillation technique (FOT), were observed after 3 hours of exposure to HVO exhaust. Our findings indicate that exposure to HVO exhaust from modern non-road vehicles at relatively low exposure levels (below the future OELs) during a short period (3 hours) can cause irritative symptoms.

Self-rated symptoms

Exposure to HVO_{PM+NOx} caused a significantly higher number of reported symptoms compared to FA, and some evidence of a similar trend for symptoms of eye and throat irritation (Table 3). In

300 addition to PM and NO_x, the HVO_{PM+NOx} exposure also contained low concentrations of VOCs such
301 as formaldehyde, BTEX and PAHs, which were not detected for HVO_{NOx}. Formaldehyde exposure
302 is a known irritant, causing eye and respiratory tract irritation (42), however, strong responses are
303 generally found at much higher concentrations (>200 µg m^{-3}, (15,43)) than used in this study
304 (HVO_{PM+NOx}: 51±6 µg m^{-3}). The mild symptoms of irritation in this study could hence be an effect
305 of the formaldehyde, despite the low concentration, in combination with the other VOCs and the
306 PM. However, the effect of NO or NO_2 alone cannot be disregarded since there were symptoms
307 reported for the HVO_{NOx} exposure as well but to a lower extent. Symptoms similar to the ones
308 observed in this study have earlier been reported by Mudway et al. (14) who found nasal, throat,
309 and eye irritation as well as bronchoconstriction in healthy volunteers exposed to petroleum diesel
310 at levels similar to the ones used in this study.
311
312 *Respiratory function*
313 Different patterns in PNIF values were found for the HVO and FA exposures (Fig. 4). In contrast to
314 FA exposure, PNIF did not increase during exposure to the HVO exhaust, hence indicating a nasal
315 obstruction during the two HVO exposures. The lack of an increase in PNIF was seen already 55
316 minutes into the exposure (Fig. 4). The decrements of ΔPNIF were larger during the HVO_{NOx}
317 exposure than during HVO_{PM+NOx} in comparison to FA (Table 1). As the HVO_{NOx} exposure did not
318 contain any PM fraction (PN<100 cm^{-3}, PM~1µg m^{-3}), the effects are attributed to the NO and NO_2
319 exposure. In addition, the larger impact on the nasal patency may be related to the NO_2 rather
320 than the NO concentration since NO was lower during the HVO_{NOx} exposure than during
321 HVO_{PM+NOx}. The 3-hour average NO_2 concentration was similar for the two HVO exposures but
322 fluctuated more for HVO_{NOx} and this caused short periods with higher concentrations (Fig. 1b).
323 However, the impact of NO_2 on nasal patency is not known, and the uptake of NO_2 generally
324 occurs deeper down in the lungs and causes effect on the small airways (44) and asthma-related
325 respiratory effects (reviewed in [45]). In this study no overall changes in lower airway function

326 (assessed with PEF, spirometry and FOT) were seen, while, for example, reduction in PEF has
327 been reported after petroleum diesel exhaust exposures of both higher (6) and lower (9) PM and
328 NO_x exposure concentrations. However, in studies with NO_2 exposures alone at similar
329 concentrations as in this study (1-3h, 0.1-4 ppm), NO_2 has not caused any significant effects on
330 lung function (assessed by spirometry) in healthy subjects (46–49).
331
332 Another cause for the increased nasal obstruction after the two HVO exposures could potentially
333 be due to local or pulmonary vasodilation induced by the NO exposure. NO is a known pulmonary
334 and systemic vasodilator, and when clinically administered it causes preferential pulmonary
335 vasodilation, which is used, for example, to treat hypoxemia and acute respiratory distress
336 syndrome (5-80 ppm) (50,51). However, as the decrement in PNIF (compared to FA) was lower for
337 HVO_{PM+NOx}, which contained higher NO than HVO_{NOx}, we cannot attribute the effect solely to NO.
338 In addition, we cannot exclude that there is an interaction effect of the PM and gases, as the
339 changes in nasal patency were less pronounced during HVO_{PM+NOx} than HVO_{NOx}.
340
341 The temporary changes in measured airway functions were small and unlikely to have clinical
342 importance in healthy persons from short-term exposure. Nevertheless, we cannot exclude a risk
343 from either short-term or long-term exposure on more sensitive persons, for example older people
344 or those with pre-existing lung or cardiovascular disease. The long-term effect of renewable diesel
345 exhaust is unknown, but the short-term responses in this study indicate that even exposure below
346 the future OELs is not completely without risk for negative health effects. Reduced PNIF is not a
347 measure of lung function, but clinically a long-term nasal obstruction caused by occupational
348 exposure could be considered indicative for the development of irritation asthma (52).
349
350 In previous studies, oscillometry measurements found early manifestations of lung disease before
351 these were measurable with spirometry (53,54). The subjects with baseline oscillometric values

352 just outside the normal range ("atypical group", Additional file A) were hence hypothesized to have
353 a different lung reaction than persons within the normal range. Differences between the
354 typical/atypical groups were investigated for oscillometric parameters, PNIF and PEF but due to
355 the small sample size, no clear conclusions can be drawn. The subjects with atypical oscillometry
356 measures showed a higher proportion of having a history of symptoms and atopy (80% vs. 54%,
357 $p<0.05$) from the initial medical assessment, which indicates that they may be more sensitive to
358 pollutants and allergens. However, studies with larger numbers of subjects need to be carried out
359 in order to draw any conclusions. It should also be noted that this group did not show any
360 indications of anomalies in the spirometry and for future controlled exposure studies, the
361 oscillometry measurement may increase the possibility to investigate small differences in lung
362 function. In addition, oscillometry may potentially be valuable in the assessment of lung function
363 effects related to occupational exposures for early detection and disease prevention.
364
365 *Aerosol characteristics, deposited dose and occupational exposure limits*
366 The total deposited mass dose of HVO_{PM+NOx} during the 3-hours exposure (82 ± 32 µg, Fig. 3b) was
367 comparable to the hourly mass dose for people working outdoor in relatively polluted cities during
368 a similar time interval (50 µg PM2.5 h^{-1}, (55)). Compared to a previous exposure study on
369 petroleum diesel (15), the HVO particles generated by the modern diesel engine in this study had a
370 smaller mobility size which caused higher deposition fractions in terms of mass, surface area and
371 number. The difference in deposition is due to the higher deposition fraction (Additional file D) of
372 smaller particles which dominated HVO_{PM+NOx} emissions (MMD 108nm) in comparison to
373 petroleum diesel (MMD 195 nm). It means that in the case of HVO_{PM+NOx}, two times more particles
374 will deposit due to their smaller size in comparison to the compared petroleum diesel particles.
375
376 Modern diesel engines utilize improved combustion parameters of, for example, increased fuel
377 injection pressure and nozzle design, which reduce the size (but not necessarily the number

concentration) of the soot particles, which in turn reduces the soot mass emissions (36). As the upcoming OEL for the EC from diesel engines is only expressed as mass (50 µg EC m^{-3}, from 2023), it may be more efficient in mitigating the inhaled and deposited dose of older diesel engine emissions, but not necessarily as efficient in reducing the deposited dose from renewable fuels and modern diesel engines without DPFs. For example, even though the PM1 mass concentration (93 µg m^{-3}) was 3 times lower for HVO in this study, compared to the previous exposure study to petroleum diesel (15) with PM1 276 µg m^{-3}, the average deposited mass (Table 2) was only a factor 0.8 lower (i.e., only 20% lower). Despite the lower PM1 mass, the number concentration was similar and the surface area even higher due to the reduced particle size. OELs in terms of particle number concentration can hence be more efficient in reducing the exposure to particle emissions from renewable fuels and modern diesel engines similar to the ones used in this study. The particle size distributions and number concentrations need to be assessed in exposure studies and not only the mass in order to understand the deposition and dose dependent effects.

Even though the EU emission standards are continuously becoming more stringent with lower allowed exhaust emissions, modern non-road vehicles lacking full emission aftertreatment systems, like the two vehicles used in this study, will still be in use and pose a risk for hazardous exposure. No vehicle in this study had an external NO_x reduction unit, and the implementation of one could potentially have reduced the NO_x emissions and related health effects. From the results in this short-exposure study, we cannot exclude the potential risk of short- and long-term effects from exposure to renewable diesel exhaust from modern non-road vehicles that comply with the latest emission standards and the future OELs.

Conclusion

We investigated the effects on airway function after exposure to exhaust from renewable diesel fuel HVO from modern vehicles in comparison to filtered air. The vehicles were manufactured in 2019

404 and complied with the current non-road engine EU emission standards. The exposure levels were
405 kept below the EU OELs. Mild irritations symptoms (self-rated) were reported during the two
406 HVO exposures, with a slightly higher incidence number during the exposure from the vehicle
407 without an aftertreatment system (HVO_{PM+NOx}). The data also suggested that some individuals
408 might be affected by exposure to HVO exhaust from modern work vehicles below the future EU
409 OELs. Compared to older diesel exhaust exposures, the deposited fraction in the respiratory tract
410 of HVO exhaust PM was higher, in terms of mass, number and surface area. The increase in
411 deposition was due to the smaller soot particle size.
412
413 In this study, the focus was on nasal patency and pulmonary function assessments. However, to
414 understand the full potential health effects of HVO exposures, additional analyses of the
415 inflammatory and cardiovascular effects need to be performed. Additionally in this study, only the
416 effects of short-term exposure to HVO exhaust were explored. This means that any conclusions
417 about the long-term effects and effects on potentially sensitive groups need to be addressed in
418 future studies.
419
420 Although the HVO fuel is more sustainable from a climate perspective, our study indicates that
421 from a health perspective, the exposure levels need to be as carefully controlled as they are for
422 petroleum diesel.
423

424 **Method**

425 **Study design**

426 In total 19 volunteers (9 f /10 m, age 20-55 years) were exposed to the two types of engine
427 emissions and particle free air during three separate 3-hour long sessions at least one week apart.
428 The exposure scenarios discussed in this publication were: 1) emissions from a wheel loader
429 without exhaust aftertreatment operated with HVO (HVO_{PM+NOx}), 2) emissions from a wheel

430 loader with an aftertreatment system operated with HVO (HVO_{NOx}), and 3) filtered air (FA). We
431 would like to point out that the whole study also included an additional exposure scenario, namely,
432 exposure to aerosolized dry NaCl, the analysis and comparisons of which will be presented
433 separately. The exposures took place in a 22 m^3 stainless steel chamber with controlled relative
434 humidity, temperature and ventilation. The study was double-blind and a maximum of four
435 participants were exposed at the same time. All exposures took place on Tuesdays, Wednesdays
436 and Thursdays, between 9-12 a.m., with a minimum of one week between each exposure. Before
437 and immediately after each exposure, the participants went through medical examinations that
438 included spirometry and used the forced oscillation technique (FOT). Self-rated symptoms, PEF
439 (peak expiratory flow) and PNIF (peak nasal inspiratory flow) were registered four times: one time
440 before and three times during the exposure (Table 7).
441
442 Table 7. Scheduling and time points of the reported measurements and self-rated symptoms.

Item	Before exposure	During exposure (time after exposure start in minutes)*			Immediately after exposure
Time point	1	2	3	4	5
Self-rated symptoms	X	35 min	95 min	155 min	
Peak Nasal Inspiratory Flow (PNIF)	X	55 min	115 min	175 min	
Peak Expiratory Flow (PEF)	X	55 min	115 min	175 min	
Spirometry	X				X
Airway Oscillometry (Forced Oscillation Technique, FOT)	X				X

* The exposure lasted 3 hours (180 minutes).

443
444 *Study population*
445 Volunteers were recruited via Lund University online channels and posters. Of the 25 volunteers
446 who underwent the initial medical examination, 19 fulfilled the inclusion criteria and were
447 consecutively selected for the study. The inclusion criteria were the following: men or non-
448 pregnant women; 20-65 years old; no known lung disease; no asthma diagnosis; normal standard
449 ECG reading; no medication that would affect the monitored parameters; non-smoker the last

450 three years. All except one of the selected participants underwent all three exposures. One person
451 only participated in the exposure to HVO_{NOx}. Characteristics of the study group are summarized in
452 Table 8. The study was approved by the Swedish Ethical Review Authority (registration no. 2019-
453 03320) and performed in accordance with the Declaration of Helsinki.
454
455 Table 8. The participants' medical history and results from the initial medical examinations before
456 commencement of the study.

		Subjects (N=19)
	Age (median, min-max)	29 (20-55)
	Female (N, %)	9 (47%)
	Previous smoker (N, %)*	7 (37%)
Medical history	History of any symptoms last 12 months (N, %)	7 (37%)
	- Eye symptoms (N, %)	1 (5%)
	- Nasal symptoms (N, %)	3 (16%)
	- Dry cough (N, %)	0
	History of chronic bronchitis (N, %)	0
	History of bronchial hyperreactivity (N, %)	5 (26%)
History of childhood atopy	Atopic dermatitis/Childhood eczema (N, %)	3 (16%)
	Allergic rhinitis/Hay fever (N, %)	1 (5%)
	Urticaria (N, %)	1 (5%)
	Physician-diagnosed asthma during childhood (N, %)	1 (5%)
Atopy	Phadiatop positive (N, %)	7 (37%)
Baseline spirometry (prior to bronchodilation)	FVC % pred. (median, min-max)	92 (70-106)
	FEV_1 % pred. (median, min-max)	94 (73-108)
	FEV_1/FVC % pred. (median, min-max)	100 (90-108)
Baseline spirometry (after bronchodilation)	FVC % pred. (median, min-max)	95 (72-107)
	FEV_1 % pred. (median, min-max)	97 (79-109)
	FEV_1/FVC % pred. (median, min-max)	100 (90-112)

*All test subjects were currently non-smokers.
FVC = forced vital capacity, FEV_1 = forced expiratory volume in one second.

457
458

Aerosol generation

The exposures took place in a 22 m^3 stainless steel chamber with an air exchange rate of 4 exchanges/hour. The supply air used for dilution was filtered from particles with a HEPA (high-efficiency particulate absorbing) filter and from gases with an active carbon filter. The temperature was kept at 26±1°C and the relative humidity at 33±4%.

Renewable diesel exposure

The renewable diesel exhaust exposure scenarios were generated with two types of modern off-road diesel vehicles with different net power (kW). Both vehicles were manufactured in 2019 and complied with the current EU emission legislation. The smaller vehicle, net power 23 kW, followed emission standard Stage IIIa (2007), and the larger vehicle with a net power of 55.4 kW followed Stage V (2019). The smaller vehicle was not equipped with any external exhaust aftertreatment (hereafter denoted HVO_{PM+NOx}), while the larger vehicle was equipped with a diesel oxidation catalyst (DOC) and a diesel particulate filter (DPF) (hereafter denoted HVO_{NOx}).

The vehicles were operated switching between load (lifting the fork and applying increased power) and idle with 15-minute intervals. During load, the vehicles were kept running around 1800-1900 rpm and during idle around 900 rpm. Both vehicles were run on 100% HVO. The exhaust was extracted from the exhaust pipe of the vehicle, transported in heated tubing and diluted in two steps: first to approximately 1:20-1:30 (heated to 30°C), and then to a total dilution ratio of 1:160 in the chamber. The setup was previously described by Wierzbicka et al. (15).

Filtered air

The filtered air (FA) exposure was obtained by provision of air that passed through a HEPA filter and an active carbon filter. The particle number concentration in the size range 0.02-2.5 µm was on average 71±43 cm^{-3}, and the volatile organic compound (VOC) concentration <10 ppb. The FA was used for comparison as a reference exposure.

485

486 # Emission characterization

487

488 ## Online characterization

489 The concentrations of PM2.5 mass, NO, and NO_2 were monitored online during the exposures to
490 keep levels below the pre-determined exposure limits of 150 µg m^{-3}, 1 ppm and 2.5 ppm,
491 respectively. The online PM2.5 mass concentration was monitored by an ambient particulate
492 monitor (TEOM series 1400a, Rupprecht & Patashnick Co., N.Y., U.S.A.). NO and NO_2 was
493 measured with a chemiluminescence analyzer (CLD 700 AL, ECO PHYSICS AG, Switzerland). The
494 raw gas emissions were measured with a flue gas analyzer (Testo 350, Testo AG, Germany) in
495 order to monitor the operation of the vehicles and to ensure exposures below hazardous CO
496 exposure levels (exposure averages were kept below 3 ppm). The CO_2 concentration in the
497 chamber was monitored with a non-dispersive infrared CO_2 analyzer (LI-8020, LI-COR, Lincoln,
498 NB, U.S.A.) and kept below 1500 ppm. The total VOC concentration (range 10-20 000 ppb) was
499 measured by an online photo-ionization technique (VelociCalc, model 9565-P, probe 986, TSI Inc.,
500 U.S.A.).

501

502 *Particle number size distribution and number concentration*

503 The particle number size distributions in the range 9.8-430 nm (HVO exposures) or 19-914 nm
504 (FA exposures) were measured with a scanning mobility particle sizer (SMPS), including an
505 electrostatic classifier (TSI model 3082) and condensation particle counter (CPC, model 3775,
506 TSI). The aerodynamic size distribution of 0.5-20 µm was monitored with an aerodynamic particle
507 sizer (APS, model 3321, TSI) during the exposures to ensure that the particle number size
508 distributions maxima were captured with the SMPS.

509

510 *Effective density (DMA-APM)*

The particle effective density was assessed using an aerosol particle mass analyzer (APM 3600, Kanomax) in combination with a differential mobility analyzer (DMA, TSI Inc., U.S.A.) and a condensation particle counter (CPC, model 3075, TSI Inc., U.S.A.) (56). The effective density was measured at five DMA-selected particle mobility diameters: 50, 70, 100, 150 and 300 nm. Mobility size (d_p) selection was performed with the DMA. The APM measured the mass distribution of the selected monodisperse aerosol by stepping the voltage for a constant rotating speed. The effective density, $\rho_{eff,}$, was derived from the arithmetic mean of the measured APM voltage-number distribution and polystyrene latex spheres (PSL, Polymer Microspheres, Duke Scientific Corporation) reference data as described by McMurry et al. (56), shown in Eq. (1):

$$\rho_{eff} = \rho_{PSL} \frac{V_{APM}}{V_{APM,PSL}} \quad (1)$$

Where ρ_{PSL} is the density of the PSL reference particles, V_{APM} is the measured arithmetic mean voltage of the sampled particles for a given mobility diameter and RPM, and $V_{APM,PSL}$ is the theoretically calculated arithmetic mean voltage of the PSL reference particles for a given mobility diameter and RPM. The DMA-APM system was calibrated with spherical PSL particles with a known density of 1.05 g cm^{-3}.

The effective density of the HVO_{PM+NOx} (soot particles) was fitted assuming a power law function, Eq. (2) (57), where C'' is a constant and D_{fm} the mass-mobility exponent.

$$\rho_{eff} = C'' d_p^{D_{fm}-3} \quad (2)$$

The mass-mobility relationship was used to extrapolate a power law function for the mobility equivalent particle diameters below 50 nm (up to the inherent material density of soot of 1.8 g cm^{-3}) and above 300 nm.

Particle mass and surface area size distribution

535 Mass size distributions were calculated by following Eq. (3), utilizing the particle number size
536 distribution (from the SMPS) and the experimentally determined effective density (ρ_{eff}, from the
537 APM) as a function of electrical mobility size (d_p).

538 $$dM/dlogd_p = \frac{\pi d_p^3}{6} * \quad \rho_{eff}(d_p) * dN/dlogd_p \qquad (3)$$

539 Lognormal distributions were fitted to the mass size distribution up to 1 µm (PM1).
540
541 The surface area (SA) distributions were calculated using the model described by Rissler et al. (39),
542 which is based on DMA-APM measurements. From the DMA-APM, the mass of individual
543 agglomerates as a function of mobility particle size can be extracted if the effective density follows
544 the soot power law function (Eq. 2). The surface area of individual agglomerates is then calculated
545 by division of the mass of the agglomerate by the primary particle mass and surface area
546 ($SA_{pp}=6/(\rho_{pp}*d_{pp})$)(39). The primary particle size (d_{pp}) is obtained from TEM images, and the
547 inherent material density of soot (1.8 g cm^{-3}) used for the primary particle density (ρ_{pp}). From the
548 surface area of individual agglomerates as a function of mobility particle size, the particle number
549 distribution (from the SMPS) can be converted to a particle surface area distribution. This method
550 accounts for the agglomerated soot structure and is described in more detail by Rissler et al. and
551 Wierzbicka et al. (15,39).
552
553 **Offline characterization**
554
555 *Gravimetric analysis*
556 The PM1 mass concentration was determined by gravimetric analysis performed by the Division of
557 Occupational and Environmental Medicine at Örebro University, Örebro, Sweden. The samples
558 were collected during the entire duration of the exposure (180 minutes) using a PM1 cyclone pre-
559 separator on 37 mm Teflon filters (Zefluor, pore size 1.0 µm) with a flow rate of 5 L min^{-1}. The

560 filters were conditioned for 48 hours at 50±3% RH and 20±1°C and weighed before and after
561 collection.
562
563 *Thermal optical carbon analysis and TEM imaging*
564 Samples for the thermal optical analysis of organic carbon (OC) and elemental carbon (EC) were
565 collected on quartz filters (47 mm, Pallflex Tissuequartz) and analyzed with a thermal optical
566 analyzer (DRI Model 2001 OC/EC Carbon Analyzer, Atmoslytic Inc., U.S.A.) using the NIOSH
567 NMAM 5040 diesel exhaust protocol. The limit of detection for EC (LOD) was 0.06 μg C cm^{-2}. Two
568 samples were collected in parallel, where one filter collected particle-free air after a Teflon filter
569 (Zefluor, pore size 1.0 μm) which was used to account for gas adsorption artifacts of the filter. Both
570 samples were collected after a PM1 cyclone at a flow rate of 5 L min^{-1} during the entire exposure
571 duration (180 min) and stored refrigerated (+6°C) until analysis.
572 To analyze the soot particle aggregate structure (morphology and primary particle size), samples
573 were collected with electrostatic precipitation using a nanometer aerosol sampler (model 3089, TSI)
574 on lacey carbon coated Cu-grids and analyzed with a transmission electron microscope (TEM, JEOL
575 3000F). The TEM was operated at 300kV and equipped with a Schottky FEG and 2x2k CCD. An
576 overview of the samples was first imaged at 10,000X magnification in order to ensure that the
577 sample was reasonably homogenous. The TEM images of HVO_{PM+NOx} were analyzed for primary
578 particle size determination with the ImageJ software (58). The diameters of the clear primary
579 particles without overlap at the edges of the soot agglomerates were measured in TEM images with
580 a magnification minimum of 25,000X. The diameters of 81 primary particles were measured from
581 10 agglomerates.
582
583 *PAH analysis*
584 Samples for particulate PAH analysis were collected at a flow rate of 2 L min^{-1} during the entire
585 exposure duration (180 minutes) on Teflon filters (diameter 37 mm, pore size 2 μm (Teflo, Pall

586 Corporation, Port Washington, N.Y., U.S.A.). These filters were followed by XAD-2 tubes (SKC
587 Inc.) for sampling of gaseous PAHs. The samples were stored at -18°C prior to analysis. The
588 samples were analyzed for 33 native and alkylated PAHs (including the 16 U.S. EPA priority
589 PAHs), 17 nitrated, 10 oxygenated PAHs (nitro-PAHs and oxy-PAHs), and 6 dibenzothiophenes
590 (DBTs), as described by Gren et al. 2020 (22). In short, prior to extraction two labelled internal
591 standard mixtures containing 16 deuterated U.S. EPA priority PAHs were spiked to the filters and
592 XAD-2 adsorbent, respectively. Samples were extracted with 3 mL dichloromethane, cleaned using
593 silica columns and concentrated to a final volume of approximately 30-40 µL. Target compounds
594 were separated on an Agilent 5975C mass spectrometer (MS) coupled to a 7890A gas
595 chromatograph (GC, Agilent Technologies, Santa Clara, CA, U.S.A.). The MS was operated in
596 selected ion monitoring mode (SIM), and electron impact ionization (EI) was performed for PAHs
597 and alkylated PAHs.
598
599 *Formaldehyde and BTEX analysis*
600 Accredited formaldehyde analysis was performed by the Division of Occupational and
601 Environmental Medicine at Örebro University, Örebro, Sweden. The samples for formaldehyde
602 analysis were collected with a flow rate of 0.2 L min^{-1} during the entire duration of the exposures
603 (180 min) on Sep-Pak DNPH-silica cartridges (Waters). 2,4-dinitrophenylhydrazine (DNPH)
604 formed derivates with aldehydes and were extracted in acetonitrile. The extracted samples were
605 analyzed with liquid chromatography ultraviolet mass spectrometry (LC-UV/MS) at wavelength
606 360 nm. The samples were stored at -18°C prior to analysis.
607
608 An accredited analysis of benzene, toluene, ethyl benzene, m+p xylene and o-xylene (BTEX) was
609 performed by the IVL Swedish Environmental Research Institute, Gothenburg, Sweden. n-butyl
610 acetate, n-octane and n-nonane were also analyzed but not included in the total BTEX
611 concentration. The samples were collected on thermal desorption tubes (TENAX TA) and analyzed

612 by a thermal desorption GC-MS method. The sorbent tubes were heated to 250°C under a helium
613 flow for 5 minutes. The emitted compounds were refocused with a cold trap (-30°C) and then
614 quickly heated to 300°C in the thermal desorption instrument (Unity2 and Ultra, Markes) and
615 injected into the GC-MS (ThermoFisher Scientific). Target compounds were separated on a non-
616 polar capillary column (TraceGold, TG-1MS, ThermoFisher Scientific) coupled to a mass
617 spectrometer (ISQ LT, ThermoFisher Scientific).
618

619 ## Model for particle deposition in the respiratory tract

620 Regional respiratory tract particle deposition fractions from nasal breathing were calculated for
621 the inhaled aerosols with the multiple-path particle dosimetry model (MPPD model version 3.04,
622 (59)). The input parameters are summarized in Table 9.
623

624 Table 9. The input parameters for the MPPD model used for estimating the respiratory tract
625 particle deposition.

MPPD model input data		HVO_{PM+NOx}	Diesel (Wierzbicka et al. [2014])
	Model	Yeh/Schum Symmetric	
	Functional residual capacity[a] (mL) (median, min-max)	3200 (2680-3750)	
	Upper respiratory tract volume (mL)	50	
Particle properties*	Density at MMD (g cm^{-3})	0.84	0.42
	PM1 mass (µg m^{-3}) (average ± 1 std. dev.)	93 ± 13	276 ± 56
	Mass Median Diameter (MMD) (µm)	0.108	0.195
	GSD	1.48	1.65
Exposure scenario	Inhalability adjustment	No	
	Acceleration of gravity (m s^{-2})	9.81	
	Body orientation	Upright	
	Breathing frequency[b] (min^{-1}) (median, min-max)	17.1 (13.3-24.9)	
	Tidal volume[c] (mL) (median, min-max)	875 (440-1500)	
	Inspiratory fraction	0.5	
	Breathing scenario	Nasal	

The aerosol characteristics from a previous diesel exposure study (15) were included and used in the MPPD model to compare the respiratory deposition of HVO and petroleum diesel. The MPPD model's reference values from ICRP (60) for upper respiratory tract volume and inspiratory fraction were used.
* Properties from the exposure aerosol characterization. [a] Calculated by height, age and sex following the guidelines of the European Respiratory Society (61). [b] Measured with a Noxturnal 5.1 breathing belt (Nox

Medical, ResMed). [c] Measured by a forced oscillometry technique with the Tremoflo (THORASYS, Thoracic Medical System Inc., Montreal, Canada).

The inhaled and deposited dose from oral breathing during the HVO_{PM+NOx} exposure was also calculated. This was done with the experimental model reported by Rissler et al. (39) to allow for comparison with a previous exposure study of petroleum diesel exhaust, where this model was used, and was performed with the same exposure setup (15).

Medical assessment

Nasal patency and pulmonary function measures

Assessment of nasal patency was performed with measurements of peak nasal inspiratory flow (PNIF) using an inspiratory flow meter (In-check, Clement Clarke International Ltd., U.K.) according to the manufacturer's instructions. Three recordings at each time point (Table 7) were performed and the highest value was used for analysis (62). The PNIF measurements were compared to the baseline value before the exposure on an individual basis, and a decrease in PNIF indicated an increased nasal obstruction (63).

Lower airway function was assessed with measurements of peak expiratory flow (PEF) measured with a MINI Wright Flow Meter (Clement Clarke International Ltd., U.K.), measuring range of 60-800 L/min. Three recordings at each time point (Table 7) were performed and the highest value was used for analysis (64). The PEF measurements were compared to the baseline value before the exposure on an individual basis, and a decrease in PEF was used as an indication of lower airway obstruction.

Spirometry was performed with SPIRARE 3 (DIAGNOSTICA, Oslo, Norway) according to the European Respiratory Society Guidelines (64). Forced vital capacity (FVC), forced expiratory flow

650 in the first second (FEV_1), FEV1/FVC, and z-scores were obtained and compared according to the
651 reference of the Global Lung Initiative (65).
652
653 Measures of oscillometry (resistance [R], reactance [X]) were obtained in a frequency range of 5-19
654 Hz by the forced oscillometric technique (FOT), with a Tremoflo (THORASYS, Thoracic Medical
655 System Inc., Canada) according to the manufacturer's instructions (40). The resistance at 5 and 19
656 Hz (R_5, R_{19}), reactance at 5 Hz, area under the reactance curve from 5 to 19 Hz (A_X), and the
657 resonant frequency (F_{res}) before all exposures were averaged and summarized for all volunteers in
658 Additional file A. The individual oscillograms were evaluated by a trained physician. Some
659 volunteers had FOT values deviating from the normal range (40,41) but with normal spirometry
660 measures, thus the volunteers were further categorized into a "typical" and "atypical" group based
661 on their oscillometric measurements. The criteria were as follows: $R_{5\text{-}19} \geq 0.8$ cmH_2O s L^{-1}, $X_5 \leq$ -
662 1.8 cmH_2O s L^{-1}, and $A_x \geq 14$ cmH_2O L^{-1} (Additional file A). These criteria were based on
663 characteristics of healthy and asthmatic subjects as published by Eddy et al. (41). The atypical
664 group showed a higher proportion of having a history of symptoms and atopy (80% vs. 54%,
665 $p<0.05$). They were hypothesized to be more sensitive and to have a different lung reaction than
666 the typical group, which was explored further in the analyses.
667
668 *Self-rated symptoms*
669 Similar to a previous study (6), self-rated symptoms of eye irritation, nose irritation (including
670 runny nose and nasal congestion), throat irritation and chest tightness/breathlessness were rated
671 by the volunteers themselves on a visual analog scale (VAS) (range 0 to 100 millimeter) before
672 exposure, and at 35, 95 and 155 min into the exposure during each exposure session (Table 7).
673
674 **Statistical analysis**

675 For each self-rated symptom (eye, nose, throat, and chest), when a volunteer gave a higher score
676 than before the exposure at any time during the exposure, this person was recoded as "reported
677 symptoms", otherwise, "no reported symptoms". A person was then recoded as "reported any
678 symptom" if he/she reported any of the four symptoms during the exposure. The calculation was
679 performed for each exposure scenario separately. Descriptive analysis was used to count the
680 number of persons and corresponding proportion of persons with reported symptoms during
681 exposure for each exposure scenario. An χ^2-test was used to investigate the difference in
682 proportion between the given exposure scenarios (each of the two exposure scenarios) in
683 comparison to FA exposure when applicable.
684
685 For PNIF and PEF measurements that were performed three times during each exposure, absolute
686 changes from before exposure were calculated on the individual level for each exposure scenario at
687 each time point. Linear mixed models were used to analyze the average changes in the selected
688 outcomes at given exposure scenarios versus changes at FA exposure. Subject ID, the exposure
689 scenarios and time points (1-4) were used to identify repeated measurements, and all models
690 included a random slope. The models further included exposure order (e.g., first or second time in
691 the chamber) as an adjustment since the order was imbalanced and a learning effect on the
692 measurement performance might have occurred.
693 For spirometry and FOT measurements, which were only performed before and after exposure, the
694 Wilcoxon signed-rank test was used to compare the differences between before and after exposure
695 at each exposure scenario.
696
697 Additionally, interaction terms between exposure scenarios and typical/atypical groups were
698 tested for PNIF, PEF and with the FOT in the linear mixed models described above, to see if the
699 atypical group with FOT measurements outside the normal range (Additional file A) showed
700 different exposure-related changes in nasal patency and pulmonary function. If the interaction

701 terms had a p-value <0.05, further stratified analyses were performed in each group for selected
702 outcomes.
703
704 All statistical analyses were performed using IBM SPSS Statistics 26. For all tests, p-values <0.1
705 were considered as weak indications, while P values <0.05 were generally accepted as significant.
706

707 Declarations

708

709 **Acknowledgements**

710 The authors thank Anders Olsson for practical help with vehicle maintenance. Panu Karjalainen is
711 acknowledged for support with initial vehicle tests. Yuliya Omelekhina is acknowledged for
712 practical help with aerosol sample collection. Madeleine Petersson and Veronica Ideböhn are
713 acknowledged for contributions to composing the ethical application.

714

715 **Authors' contributions**

716 Original project idea and obtaining funding: AG and AW. Exposure scenarios design: AW and LG.
717 Project management and coordination of exposures: AW. Aerosol generation: LG, JP, AW, AG.
718 Initial test and selection of vehicles: LG, JP. Aerosol instrument data collection: LG, FM. Aerosol
719 instrument data analysis and lung deposition analysis: LG. TEM images and analysis: LG. Carried
720 out the experiments: LG, KD, EA, JN, FM. Vehicle operation: FM. PAH analysis: AMK, BS. OCEC
721 analysis: KL. Medical assessment and measurements: KD, EA, JN. FOT data analysis and
722 interpretation: LG, KD, PW. Statistical analysis: YX. Health effects/medical data interpretation:
723 LG, KD, MK, MA, JN, AW, AG, JL. LG wrote the manuscript and conceived the figures. All co-
724 authors contributed to critical revisions of the manuscript. All co-authors will have approved the
725 final manuscript.
726

Funding

This research was financed by the Swedish Research Council FORMAS (2016-00824). Jakob Löndahl acknowledges funding from the Swedish Research Council for Health, Working Live and Welfare FORTE (project number 2017-00690).

Availability of data and materials

The datasets used and/or analyzed during the current study are available from the corresponding author on reasonable request.

Ethics approval and consent to participate

The study was approved by the Swedish Ethical Review Authority (registration no. 2019-03320) and performed in accordance with the Declaration of Helsinki and included obtaining informed written consent.

Consent for publication

Not applicable

Competing interests

The authors declare that they have no competing interests.

Abbreviations

APM	aerosol particle mass analyzer
BTEX	benzene, toluene, ethyl benzene, m+p xylene, o-xylene
CI	confidence interval
DMA	differential mobility analyzer
DPF	diesel particle filter

DOC	diesel oxidation catalyst
EC	elemental carbon
FA	filtered air
FEV	forced expiratory volume
FOT	forced oscillation technique
FVC	forced vital capacity
HVO	hydrotreated vegetable oil
MMD	mass median diameter
MPPD	multiple-path particle dosimetry model
NO	nitrogen monoxide
NO_2	nitrogen dioxide
NO_x	nitrogen oxides
OELs	occupational exposure limits
PAHs	polycyclic aromatic hydrocarbons
PEF	peak expiratory flow
PM	particulate matter
PN	particle number
PNIF	peak nasal inspiratory flow
SA	surface area
TEM	transmission electron microscope
VAS	visual analog scale
VOC	volatile organic compound

References

1. Hesterberg TW, Long CM, Lapin CA, Hamade AK, Valberg PA. Diesel exhaust particulate (DEP) and nanoparticle exposures: What do DEP human clinical studies tell us about

779 potential human health hazards of nanoparticles. Inhal Toxicol. 2010;22(8):679–94.
780 2. Ris C. U.S. EPA Health assessment for diesel engine exhaust: A review. Inhal Toxicol.
781 2007;19(SUPPL. 1):229–39.
782 3. Riedl M, Diaz-Sanchez D. Biology of diesel exhaust effects on respiratory function. J Allergy
783 Clin Immunol. 2005;115(2):221–8.
784 4. Sydbom A, Blomberg A, Parnia S, Stenfors N, Sandström T, Dahlén S-E. Health effects of
785 diesel exhaust. Clin Occup Environ Med. 2003;3(1):61–80.
786 5. IARC. Diesel and Gasoline Engine Exhausts and Some Nitroarenes. Vol. 105, IARC
787 monographs on the evaluation of carcinogenic risks to humans. 2014.
788 6. Xu Y, Barregard L, Nielsen J, Gudmundsson A, Wierzbicka A, Axmon A, et al. Effects of
789 diesel exposure on lung function and inflammation biomarkers from airway and peripheral
790 blood of healthy volunteers in a chamber study. Part Fibre Toxicol. 2013;10(1):1–9.
791 7. Rudell B, Ledin MC, Hammarström U, Stjernberg N, Lundbäck B, Sandström T. Effects on
792 symptoms and lung function in humans experimentally exposed to diesel exhaust. Occup
793 Environ Med. 1996;53(10):658–62.
794 8. Mehus AA, Reed RJ, Lee VST, Littau SR, Hu C, Lutz EA, et al. Comparison of acute health
795 effects from exposures to diesel and biodiesel fuel emissions. J Occup Environ Med.
796 2015;57(7):705–12.
797 9. Andersen MHG, Frederiksen M, Saber AT, Wils RS, Fonseca AS, Koponen IK, et al. Health
798 effects of exposure to diesel exhaust in diesel-powered trains. Part Fibre Toxicol.
799 2019;16(1):1–14.
800 10. Stenfors N, Nordenhäll C, Salvi SS, Mudway I, Söderberg M, Blomberg A, et al. Different
801 airway inflammatory responses in asthmatic and healthy humans exposed to diesel. Eur
802 Respir J. 2004;23(1):82–6.
803 11. Salvi S, Blomberg A, Rudell B, Kelly F, Sandström T, Holgate ST, et al. Acute inflammatory
804 responses in the airways and peripheral blood after short-term exposure to diesel exhaust in

805 healthy human volunteers. Am J Respir Crit Care Med. 1999;159(3):702–9.
806 12. Salvi SS, Nordenhall C, Blomberg A, Rudell B, Pourazar J, Kelly FJ, et al. Acute exposure to
807 diesel exhaust increases IL-8 and GRO-α production in healthy human airways. Am J Respir
808 Crit Care Med. 2000;161(2 I):550–7.
809 13. Behndig AF, Mudway IS, Brown JL, Stenfors N, Helleday R, Duggan ST, et al. Airway
810 antioxidant and inflammatory responses to diesel exhaust exposure in healthy humans. Eur
811 Respir J. 2006;27(2):359–65.
812 14. Mudway IS, Stenfors N, Duggan ST, Roxborough H, Zielinski H, Marklund SL, et al. An in
813 vitro and in vivo investigation of the effects of diesel exhaust on human airway lining fluid
814 antioxidants. Arch Biochem Biophys. 2004;423(1):200–12.
815 15. Wierzbicka A, Nilsson PT, Rissler J, Sallsten G, Xu Y, Pagels JH, et al. Detailed diesel
816 exhaust characteristics including particle surface area and lung deposited dose for better
817 understanding of health effects in human chamber exposure studies. Atmos Environ.
818 2014;86:212–9.
819 16. Lundbäck M, Mills NL, Lucking A, Barath S, Donaldson K, Newby DE, et al. Experimental
820 exposure to diesel exhaust increases arterial stiffness in man. Part Fibre Toxicol. 2009;6:1–
821 6.
822 17. Mills NL, Törnqvist H, Gonzalez MC, Vink E, Robinson SD, Söderberg S, et al. Ischemic and
823 thrombotic effects of dilute diesel-exhaust inhalation in men with coronary heart disease. N
824 Engl J Med. 2007;357(11):1075–82.
825 18. Langrish JP, Bosson J, Unosson J, Muala A, Newby DE, Mills NL, et al. Cardiovascular
826 effects of particulate air pollution exposure: Time course and underlying mechanisms. J
827 Intern Med. 2012;272(3):224–39.
828 19. Lapuerta M, Armas O, Rodríguez-Fernández J. Effect of biodiesel fuels on diesel engine
829 emissions. Prog Energy Combust Sci. 2008;34(2):198–223.
830 20. Murtonen T, Aakko-Saksa P, Kuronen M, Mikkonen S, Lehtoranta K. Emissions with heavy-

831 duty diesel engines and vehicles using FAME, HVO and GTL fuels with and without DOC+
832 POC aftertreatment. SAE Int J Fuels Lubr. 2010;2(2):147–66.
833 21. Kuronen M, Mikkonen S, Aakko P, Murtonen T. Hydrotreated Vegetable Oil as Fuel for
834 Heavy Duty Diesel Engines. 2007;(724). Available from:
835 http://www.sae.org/technical/papers/2007-01-4031
836 22. Gren L, Malmborg VB, Jacobsen NR, Shukla PC, Bendtsen KM, Eriksson AC, et al. Effect of
837 renewable fuels and intake O2 concentration on diesel engine emission characteristics and
838 reactive oxygen species (ROS) formation. Atmosphere (Basel). 2020;11(6).
839 23. Unosson J, Kabele M, Boman C, Nyström R, Sadiktsis I, Westerholm R, et al. Acute
840 cardiovascular effects of controlled exposure to dilute petrodiesel and biodiesel exhaust in
841 healthy volunteers: A crossover study. Res Sq. 2020;1–29.
842 24. Matti Maricq M. Chemical characterization of particulate emissions from diesel engines: A
843 review. J Aerosol Sci. 2007;38(11):1079–118.
844 25. Savic N, Rahman MM, Miljevic B, Saathoff H, Naumann KH, Leisner T, et al. Influence of
845 biodiesel fuel composition on the morphology and microstructure of particles emitted from
846 diesel engines. Carbon N Y. 2016;
847 26. Knothe G, Krahl J, Van Gerpen J. The biodiesel handbook. Elsevier; 2015.
848 27. Rodríguez-Fernández J, Lapuerta M, Sánchez-Valdepeñas J. Regeneration of diesel
849 particulate filters: Effect of renewable fuels. Renew Energy. 2017;104:30–9.
850 28. Gren L, Malmborg VB, Falk J, Markula L, Novakovic M, Shamun S, et al. Effects of
851 renewable fuel and exhaust aftertreatment on primary and secondary emissions from a
852 modern heavy-duty diesel engine. J Aerosol Sci. 2021;156(November 2020):105781.
853 29. European Council. Directive (EU) 2019/130 of the European Parliament and of the Council
854 of 16 January 2019 amending Directive 2004/37/EC on the protection of workers from the
855 risks related to exposure to carcinogens or mutagens at work (Text with EEA relevance.).
856 Vol. 30. 2019.

857 30. European Council. Directive (2004/37/EC) of the European Parliament and of the Council
858 amending the Protection of Workers from the Risks Related to Exposure to Carcinogenic or
859 Mutagens at Work. Off J Eur Union. 2017;
860 31. Liu ZG, Eckerle WA, Ottinger NA. Gas-phase and semivolatile organic emissions from a
861 modern nonroad diesel engine equipped with advanced aftertreatment. J Air Waste Manag
862 Assoc. 2018;68(12):1333–45.
863 32. Zeraati-Rezaei S, Alam MS, Xu H, Beddows DC, Harrison RM. Size-resolved physico-
864 chemical characterization of diesel exhaust particles and efficiency of exhaust
865 aftertreatment. Atmos Environ. 2020;222(October 2019):117021.
866 33. Reşitoğlu IA, Altinişik K, Keskin A. The pollutant emissions from diesel-engine vehicles and
867 exhaust aftertreatment systems. Clean Technol Environ Policy. 2015;17(1):15–27.
868 34. Landwehr KR, Larcombe AN, Reid A, Mullins BJ. Critical Review of Diesel Exhaust
869 Exposure Health Impact Research Relevant to Occupational Settings: Are We Controlling
870 the Wrong Pollutants? Exposure and Health. Springer Netherlands; 2020.
871 35. Knecht W. Diesel engine development in view of reduced emission standards. Energy.
872 2008;33(2):264–71.
873 36. Hielscher K, Brauer M, Baar R. Reduction of soot emissions in diesel engines due to
874 increased air utilization by new spray hole configurations. Automot Engine Technol.
875 2016;1(1–4):69–79.
876 37. Finlay WH, Martin AR. Recent advances in predictive understanding of respiratory tract
877 deposition. J Aerosol Med Pulm Drug Deliv. 2008;21(2):189–206.
878 38. Park K, Kittelson DB, McMurry PH. Structural properties of diesel exhaust particles
879 measured by Transmission Electron Microscopy (TEM): Relationships to particle mass and
880 mobility. Aerosol Sci Technol. 2004;38(9):881–9.
881 39. Rissler J, Swietlicki E, Bengtsson A, Boman C, Pagels J, Sandström T, et al. Experimental
882 determination of deposition of diesel exhaust particles in the human respiratory tract. J

883 Aerosol Sci. 2012;48:18–33.
884 40. Lundblad LKA, Siddiqui S, Bossé Y, Dandurand RJ. Applications of oscillometry in clinical
885 research and practice. Can J Respir Crit Care, Sleep Med. 2019;0(0):1–15.
886 41. Eddy RL, Westcott A, Maksym GN, Parraga G, Dandurand RJ. Oscillometry and pulmonary
887 magnetic resonance imaging in asthma and COPD. Physiol Rep. 2019;7(1):1–12.
888 42. Arts JHE, Rennen MAJ, De Heer C. Inhaled formaldehyde: Evaluation of sensory irritation
889 in relation to carcinogenicity. Regul Toxicol Pharmacol. 2006;44(2):144–60.
890 43. Lang I, Bruckner T, Triebig G. Formaldehyde and chemosensory irritation in humans: A
891 controlled human exposure study. Regul Toxicol Pharmacol. 2008;50(1):23–36.
892 44. Sandstrom T. Respiratory effects of air pollutants: Experimental studies in humans. Eur
893 Respir J. 1995;8(6):976–95.
894 45. EPA. Integrated Science Assessment for Oxides of Nitrogen - Health Criteria. 2016.
895 46. Frampton MW, Boscia J, Roberts NJ, Azadniv M, Torres A, Christopher COX, et al. Nitrogen
896 dioxide exposure: Effects on airway and blood cells. Am J Physiol - Lung Cell Mol Physiol.
897 2002;282(1 26-1):155–65.
898 47. Frampton MW, Morrow PE, Cox C, Gibb FR, Speers DM UM. Effects of nitrogen dioxide
899 exposure on pulmonary function and airway reactivity in normal humans. Am Rev Respir
900 Dis. 1991;Mar 143(3):522–7.
901 48. Brand P, Bertram J, Chaker A, Jörres RA, Kronseder A, Kraus T, et al. Biological effects of
902 inhaled nitrogen dioxide in healthy human subjects. Int Arch Occup Environ Health.
903 2016;89(6):1017–24.
904 49. Langrish JP, Lundbäck M, Barath S, Söderberg S, Mills NL, Newby DE, et al. Exposure to
905 nitrogen dioxide is not associated with vascular dysfunction in man. Inhal Toxicol.
906 2010;22(3):192–8.
907 50. Creagh-Brown BC, Griffiths MJD, Evans TW. Bench-to-bedside review: Inhaled nitric oxide
908 therapy in adults. Crit Care. 2009;13(3):221.

909 51. Yu B, Ichinose F, Bloch DB, Zapol WM. Inhaled nitric oxide. Br J Pharmacol.
910 2019;176(2):246–55.
911 52. Shusterman D. Occupational irritant and allergic rhinitis. Curr Allergy Asthma Rep.
912 2014;14(4).
913 53. Zaidan MF, Reddy AP, Duarte A. Impedance oscillometry: Emerging role in the management
914 of chronic respiratory disease. Curr Allergy Asthma Rep. 2018;18(1).
915 54. Frantz S, Nihlén U, Dencker M, Engström G, Löfdahl CG, Wollmer P. Impulse oscillometry
916 may be of value in detecting early manifestations of COPD. Respir Med. 2012;106(8):1116–
917 23.
918 55. Hussein T, Saleh SSA, dos Santos VN, Boor BE, Koivisto AJ, Löndahl J. Regional inhaled
919 deposited dose of urban aerosols in an eastern Mediterranean city. Atmosphere (Basel).
920 2019;10(9).
921 56. McMurry PH, Wang X, Park K, Ehara K. The relationship between mass and mobility for
922 atmospheric particles: A new technique for measuring particle density. Aerosol Sci Technol.
923 2002;36(2):227–38.
924 57. Park K, Cao F, Kittelson DB, McMurry PH. Relationship between particle mass and mobility
925 for diesel exhaust particles. Environ Sci Technol. 2003;37(3):577–83.
926 58. Schneider CA, Rasband WS, Eliceiri KW. NIH Image to ImageJ: 25 years of image analysis.
927 Nat Methods. 2012;9(7):671–5.
928 59. Asgharian B, Hofmann W, Bergmann R. Particle deposition in a multiple-path model of the
929 human lung. Aerosol Sci Technol. 2001;34(4):332–9.
930 60. ICRP. Human Respiratory Tract Model for Radiological Protection. Ann ICRP 24.
931 1994;ICRP Publi:(1-3).
932 61. Stocks J, Quanjer PH. Reference values for residual volume, functional residual capacity and
933 total lung capacity: ATS Workshop on Lung Volume Measurements Official Statement of the
934 European Respiratory Society. Eur Respir J. 1995;8(3):492–506.

935 62. Ottaviano G, Scadding GK, Coles S, Lund VJ. Peak nasal inspiratory flow; normal range in
936 adult population. Rhinology. 2006;44(1):32–5.
937 63. Mo S, Gupta SS, Stroud A, Strazdins E, Hamizan AW, Rimmer J, et al. Nasal Peak
938 Inspiratory Flow in Healthy and Obstructed Patients: Systematic Review and Meta-Analysis.
939 Laryngoscope. 2021;131(2):260–7.
940 64. Graham BL, Steenbruggen I, Barjaktarevic IZ, Cooper BG, Hall GL, Hallstrand TS, et al.
941 Standardization of spirometry 2019 update an official American Thoracic Society and
942 European Respiratory Society technical statement. Am J Respir Crit Care Med.
943 2019;200(8):E70–88.
944 65. Quanjer PH, Stanojevic S, Cole TJ, Baur X, Hall GL, Culver BH, et al. Multi-ethnic reference
945 values for spirometry for the 3-95-yr age range: The global lung function 2012 equations.
946 Eur Respir J. 2012;40(6):1324–43.
947
948

Figures

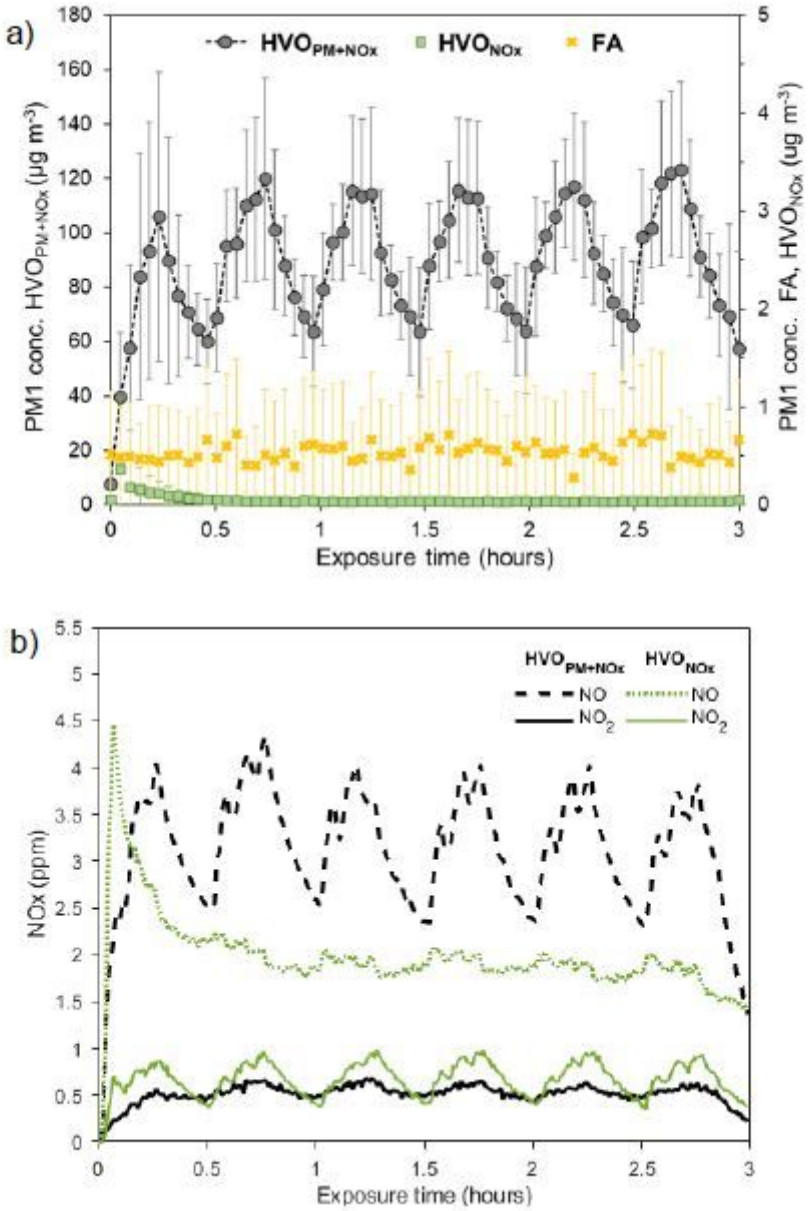

Figure 1

please see the manuscript file for the full caption

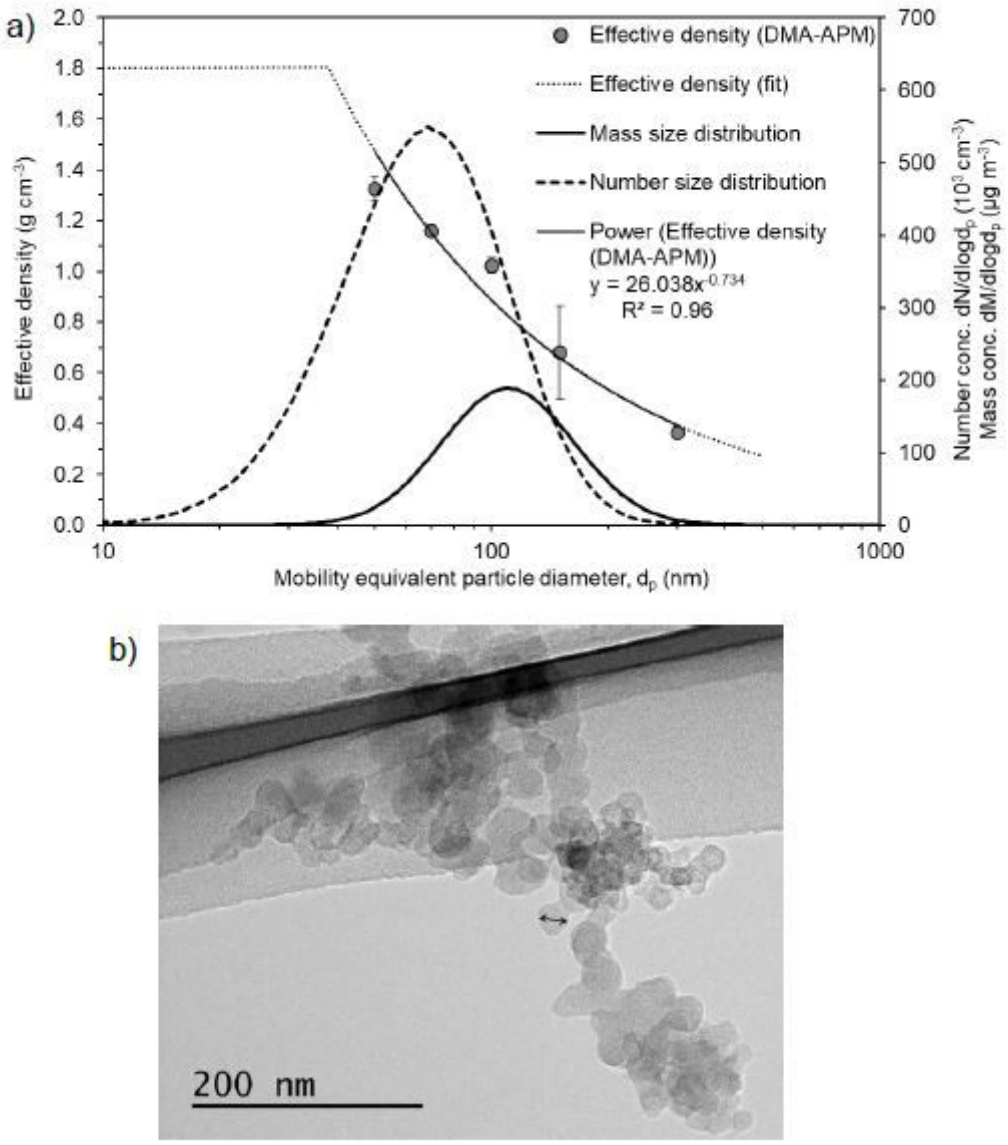

Figure 2

please see the manuscript file for the full caption

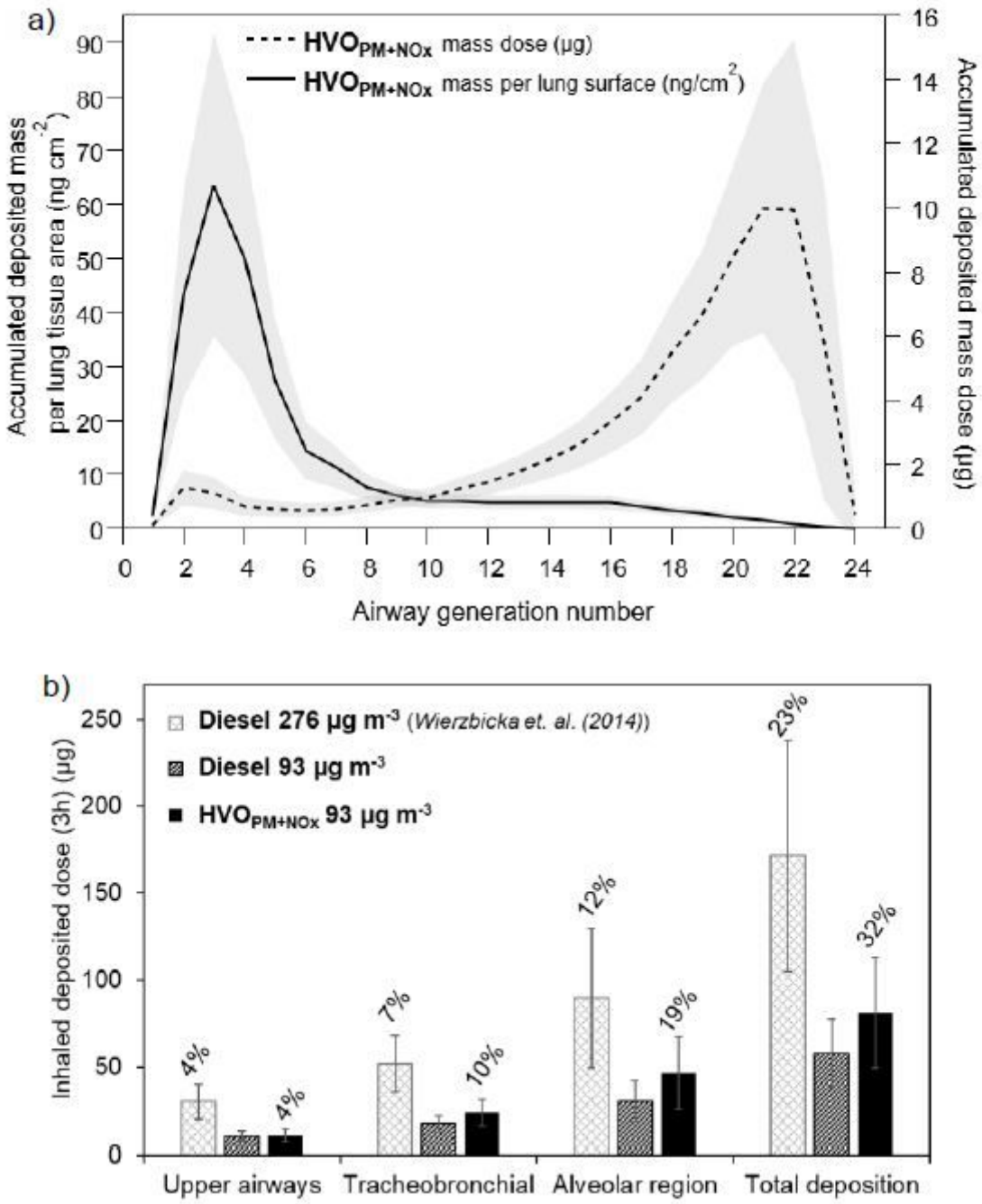

Figure 3

please see the manuscript file for the full caption

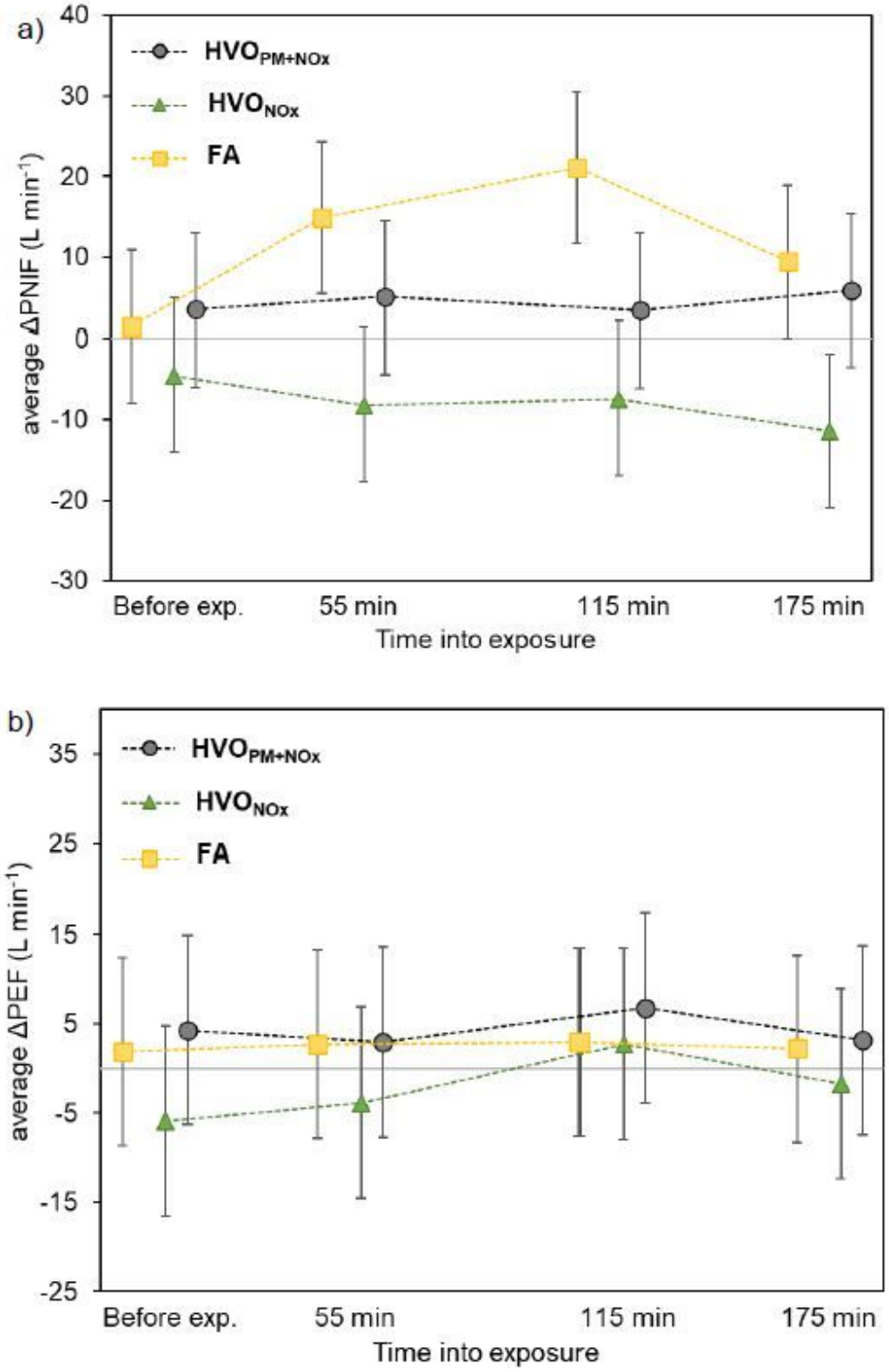

Figure 4

please see the manuscript file for the full caption

Supplementary Files

This is a list of supplementary files associated with this preprint. Click to download.

- PFTGrenetalChamber2019Additionalfile1vF.pdf